



River sediment microbial community composition and function impacted by thallium spill



Shuang Yan ^a, Zhengke Zhang ^b, Ji Wang ^b, Yulin Xia ^b, Sili Chen ^{b,*}, Shuguang Xie ^a

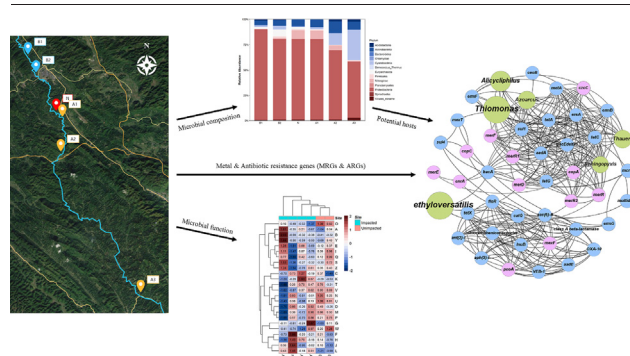
^a State Key Joint Laboratory of Environmental Simulation and Pollution Control, College of Environmental Sciences and Engineering, Peking University, Beijing 100871, China

^b South China Institute of Environmental Sciences (SCIENS), Ministry of Ecology and Environment (MEE), Guangzhou 510655, China

HIGHLIGHTS

- Thallium spill altered microbial composition and function in sediments.
- *Proteobacteria* dominated the microbial community and *Cyanobacteria* had a strong metal resistance.
- Thallium pollution played a role in screening resistance genes in the environment.
- *Sphingopyxis* was the largest potential host of resistance genes.

GRAPHICAL ABSTRACT



ARTICLE INFO

Editor: Filip M.G. Tack

Keywords:

Thallium spill
River sediment
Microbial community
Metabolic pathway
Functional genes
Resistance genes

ABSTRACT

Thallium (Tl) is widely used in various industries, which increases the risk of leakage into the environment. Since Tl is highly toxic, it can do a great harm to human health and ecosystem. In order to explore the response of freshwater sediment microorganisms to sudden Tl spill, metagenomic technique was used to elucidate the changes of microbial community composition and functional genes in river sediments. Tl pollution could have profound impacts on microbial community composition and function. *Proteobacteria* remained the dominance in contaminated sediments, indicating that it had a strong resistance to Tl contamination, and *Cyanobacteria* also showed a certain resistance. Tl pollution also had a certain screening effect on resistance genes and affected the abundance of resistance genes. Metal resistance genes (MRGs) and antibiotic resistance genes (ARGs) were enriched at the site near the spill site, where Tl concentration was relatively low among polluted sites. When Tl concentration was higher, the screening effect was not obvious and the resistance genes even became lower. Moreover, there was a significant correlation between MRGs and ARGs. In addition, co-occurrence network analysis showed that *Sphingopyxis* had the most links with resistance genes, indicating that it was the biggest potential host of resistance genes. This study provided new insight towards the shifts in the composition and function of microbial communities after sudden serious Tl contamination.

1. Introduction

Thallium (Tl), the 81st element in the periodic table, is of highly toxicity to plants, animals and human body (Peter and Viraraghavan, 2005). Tl is widely used in the field of medicine, and then it has been gradually applied

in the fields of electronics, aerospace, metallurgy, communication, health and so on (J. Liu et al., 2019). Tl is highly neurotoxic and can cause oxidative stress, resulting in cytotoxic and genotoxic effects. Excessive intake of Tl can lead to vomiting, diarrhea, injury to the heart, lung and other organs, and death in adults when they ingest only 8–10 mg/kg body mass (Campanella et al., 2019; Rodriguez-Mercado et al., 2017; Wang et al., 2022). What's more, Tl is an associated element, and the mining of major mines can lead to the release of Tl into the environment, resulting in

* Corresponding author.

E-mail address: Chensili@scies.org (S. Chen).

pollution of water, soil and gas (Karbowska, 2016). The Tl content in mine drainage water in Italy reached 30 $\mu\text{g/L}$ (the concentration in the upstream was $<0.1 \mu\text{g/L}$, and the limit for surface water in Italy was 2 $\mu\text{g/L}$) (Petrini et al., 2016), and in river water close to mining area in China it could be as high as 194.4 $\mu\text{g/L}$ (The concentration in the upstream was 0.7–0.95 $\mu\text{g/L}$, and the limit for industrial wastewater in China was 5–17 $\mu\text{g/L}$) (Belzile and Chen, 2017; Liu et al., 2017).

After being contaminated by heavy metals, the microbial community composition in aquatic sediments can shift greatly (Chen et al., 2022; Guo et al., 2019; Li et al., 2021; Wang et al., 2020). However, some specific microorganisms can show tolerance to heavy metals. The microbial groups with tolerance to specific heavy metals can be identified by comparing contaminated sites with background sites. The mechanism of microbial tolerance to heavy metals includes physiological and biochemical mechanisms as well as molecular mechanisms. Microorganisms can adsorb heavy metals through cell surface (Li et al., 2017; Xu et al., 2017) or exudate (Manasi and Rajesh, 2015; Mota et al., 2015). Moreover, microorganisms excrete (Bennett et al., 2015; Pi et al., 2016) or restore (Mahbub et al., 2016; Manasi and Rajesh, 2015) heavy metals to protect themselves from damage, and some microorganisms harbor resistance genes to resist the invasion of heavy metals. The environment polluted by heavy metals has certain screening effect on metal resistance genes (MRGs) and antibiotic resistance genes (ARGs) in microorganisms (Gupta et al., 2023; Rasool and Xiao, 2018; Sun et al., 2021).

Metagenomics technology can be used to analyze the microbial gene sequences before and after pollution, as well as to monitor the existing MRGs and ARGs, and further decipher the microbial functional changes caused by metal pollution (Chen et al., 2022, 2023). In this study, metagenomic sequencing of microorganisms in river sediment pollution caused by an accidental Tl discharge event was conducted to unveil the effects of Tl pollution on microbial community structure, metabolic pathways and functional genes in river sediments, in order to obtain more comprehensive information about microbial response to sudden accidental Tl spill.

2. Materials and methods

2.1. Study site and sampling

The environmental emergency occurred in southern China. A metal smelting enterprise discharged wastewater containing excessive Tl into the study river (River Diao). After the occurrence of the Tl spill, the Tl removal agent (coagulants polyferric sulfate and polyacrylamide) was dosed into the contaminated water.

The water and sediment samples were collected in half a month after the metal spill, and the coagulant addition was stopped at the time of sampling. Sites B1 and B2, respectively 10 km and 6 km upstream of the spill site, served as the background sites (Fig. 1). Site N was the total wastewater discharge outlet of enterprises on the River Diao, immediately downstream of the spill site. Sites A1, A2 and A3 were 0.3, 10 and 50 km downstream of the spill site, respectively.

Five-liter water harvester was used for water sampling, and the harvester was inserted 0.5 m below the surface. No air bubble was generated in the water sample during the sampling process. The whole bottle was filled with water and sealed immediately. The sampling of surface sediments (0–10 cm) was performed using a Van Veen grab sampler.

2.2. Physicochemical analysis

Water and sediment samples from the six sites at River Diao were immediately transported to the laboratory. Water pH was measured with pH meter, and total organic carbon (TOC) was determined with TOC analyzer. The determination of ammonia nitrogen ($\text{NH}_4^+ - \text{N}$) followed the Nessler's Reagent Spectrophotometry regulated by the Chinese standard protocol (HJ634-2012, the detection limit is 0.01 mg/L). Tl concentration in water was determined by inductively coupled plasma mass spectrometry (ICP-MS) (HJ700-2014, the detection limit is 0.02 $\mu\text{g/L}$). Sediment pH

was determined according to the potentiometric standard protocol (HJ962-2018). The determination of Tl concentration in sediments was carried out using ICP-MS according to the Technical Regulations for Detailed Survey of Soil Pollution in China (Environmental Office Soil Letter [2017] No. 1625, the detection limit is 0.02 mg/kg).

2.3. DNA extraction and metagenomic sequencing

DNA was extracted from 500 mg of each sediment sample using FastDNA® Spin Kit for Soil. DNA purity, concentration and integrity were determined using NanoDrop2000, Quantus Fluorometer (Picogreen) and agarose gel electrophoresis, respectively. After the PE library was constructed using TruSeq™ DNA Sample Prep Kit and bridging PCR using HiSeq 3000/4000 PE Cluster Kit, Illumina HiSeq sequencing was performed using HiSeq 3000/4000 SBS Kits.

2.4. Sequencing data analysis

The raw data was sequence quality controlled using Kneaddata (version 0.6.1) process, in which Trimmomatic (version 0.39) was used to remove adapters and low-quality reads (Bolger et al., 2014), and Bowtie2 (version 2.3.5.1) was applied to remove host sequence (Langmead and Salzberg, 2012). MetaPhlan2 was adopted for tag gene alignment and taxonomic classification (Segata et al., 2012). Megahit (version 1.2.9) was then applied to cut the reads into small fragments and reassemble to contigs (Li et al., 2015). Quast (version 5.0.2) was used to evaluate the spliced contigs (Gurevich et al., 2013), and Prokka (version 1.14.6) was used for gene annotation (Seemann, 2014). CD-HIT was then adopted to construct non-redundant gene sets and translate nucleic acid sequences into protein sequences (Fu et al., 2012), followed by Salmon for gene quantification (Patro et al., 2017).

Functional gene annotation was performed using the protein sequences, and relative abundance was calculated using quantitative results. The Diamond (version 2.0.15) pattern in emapper (version 2.1.9) (Cantalapiedra et al., 2021) was used to compare the sequences with eggNOG database (version 5.0.2) (Huerta-Cepas et al., 2019) to obtain functional genes classified by COG and KEGG. Then, the database of MRGs experimentally confirmed was selected from BacMet database (version 2.0) (Pal et al., 2014), and the SARG resistance gene database (version 2.2) (Yin et al., 2018) was adopted. The blastp pattern in diamond was applied to align protein sequences to these two databases to obtain the potential MRGs and ARGs at each site (identity ≥ 90 , e-value $\leq 10^{-10}$ and alignment length > 25).

2.5. Statistical analysis

Software R (version 4.1.2) was used for data analysis and figure drawing. Heatmaps were drawn using the pheatmap package (Kolde, 2019), and the data was scaled to make the images clearer and easier to read. Pearson correlation was performed for inter-factor correlation analysis, corrplot package (Wei and Simko, 2021) was used for visualization, and each factor was sorted using 'FPC'. For co-correlation network analysis, the psych package (Revelle, 2021) was first used for spearman correlation analysis, and the data of $r > 0.7$ and $p < 0.05$ were screened. Moreover, the igraph package (Csardi and Nepusz, 2006) was used for data statistics and preliminary drawing, and finally software Gephi (version 0.9.7) was used for drawing and modification. In addition, other figures were drawn using the ggplot2 package (Wickham, 2016).

3. Results

3.1. Physicochemical properties

Water pH decreased slightly at the spill site, and then gradually increased along with the river flow (Table 1). However, $\text{NH}_4^+ - \text{N}$ and TOC increased near the spill site but then dropped back to below the values at

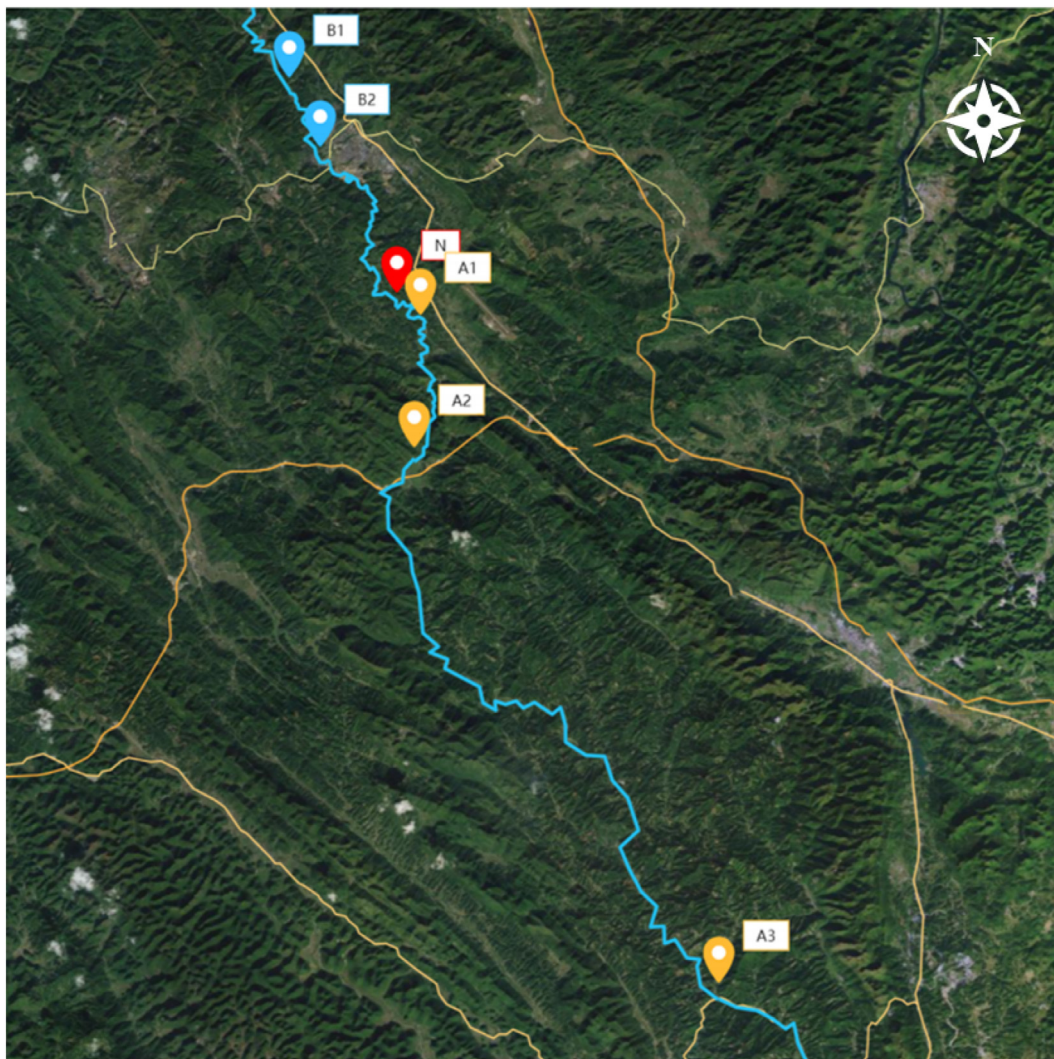


Fig. 1. Schematic diagram of sampling sites.

background sites. The water Tl concentrations at background sites B1 and B2 were lower than the maximum allowable concentration regulated by China Surface Water Environmental Quality Standard (GB3838–2002) for drinking water source (0.1 $\mu\text{g/L}$). However, water Tl contents at all spill-impacted sites much exceeded the standard. The water Tl concentration peaked at site A2 (6.46 $\mu\text{g/L}$), 323 times of that at background site B2 (0.02 $\mu\text{g/L}$). Due to the dilution of water flow, the Tl concentration at site A3 decreased to 3.32 $\mu\text{g/L}$. The change of Tl concentration in sediment was similar as that in water, but the highest value occurred at site A1 (41.5 mg/kg), 47.7 times of that at background site B2 (0.87 mg/kg). And only a slight change of sediment pH was detected.

3.2. Microbial community composition

Kingdoms of archaea, bacteria and viruses were annotated from metagenomic data. The dominant kingdom was bacteria, which made up 93.0–98.6 % of total microbial community (Fig. S1). A total of 13 phyla were noted, including one from archaea, one from viruses, and 11 from bacteria. Proteobacteria showed the highest abundance, accounting for 89.3 %, 79.1 %, 79.3 %, 79.5 %, 68.4 % and 55.5 % at sites B1, B2, N, A1, A2 and A3, respectively. The main proteobacterial classes were Alphaproteobacteria and Betaproteobacteria, respectively accounting for 16.5 %–73.6 % and 20.8 %–79.7 % of the phylum. After Tl spill,

Table 1
Physicochemical profiles of river water and sediment samples.

Site	Longitude, latitude	Water pH	Water $\text{NH}_4^+\text{-N}$ (mg/L)	Water TOC (mg/L)	Water Tl ($\mu\text{g/L}$)	Sediment pH	Sediment Tl (mg/kg)
B1	107.64130975°E, 24.87583249°N	7.85	0.04	1.95	0.06	8.36	1.14
B2	107.64953613°E, 24.86229730°N	7.84	0.02	1.68	0.02	7.83	0.87
N	107.66962051°E, 24.84130794°N	7.38	0.06	2.12	1.49	7.78	4.76
A1	107.67447363°E, 24.80931687°N	7.89	0.05	3.03	4.36	7.91	41.5
A2	107.67847703°E, 24.74307507°N	8.10	0.05	2.48	6.46	7.85	10.4
A3	107.83630371°E, 24.55461799°N	8.18	0.01	1.24	3.32	7.76	5.84

Alphaproteobacteria was enriched and even exceeded Betaproteobacteria (Fig. S2). Cyanobacteria almost disappeared near the spill site (0.6 % at site N) but then got gradually enriched in the downstream (1.9 % at site A1, 11.6 % at site A2 and 29.9 % at site A3), indicating that it had a certain degree of resistance (Fig. 2a). Clustering analysis at phylum level showed that microbial communities at sites A2 and A3 belonged to one category (Fig. 2b), while clustering analysis at genus level showed that microbial community at site A3 alone formed a category (Fig. S3). These indicated that the microbial community structure at site A3 was different from those at background sites.

At the genus level, a total of 128 genera were accurately identified, including 51 with an average relative abundance > 0.1 %. The major genera were *Thiobacillus* (1.0 %–14.4 %), *Methyloversatilis* (0.7 %–14.0 %) and *Thiomonas* (3.8 %–9.8 %), which comprised 5.8 %–31.3 % for the total microbial community. Some bacterial species were affected by T1 contamination. *Methylibium* decreased from 8.4 % at site B1 to 0.2 % at site A1, and *Thiobacillus* decreased from 14.4 % at site B2 to 5.3 % at site A1 and then 1.0 % at site A3 (Fig. 2c). Moreover, *Hyphomicrobium* (17.4 %), *Thiomonas* (9.8 %) and *Alicyclophilus* (8.1 %) predominated at site A1 (with the highest sediment T1 concentration) (Fig. 2d), which suggested that these genera might have T1 resistance.

3.3. Functional composition

COG functional classification of sequences was performed using the eggNOG database. Similar to the microbial community composition at the genus level, COG clustering analysis revealed that functional composition at site A3 alone formed a category and was different from those at other sites (Fig. S4). At all sites, functions ‘Energy production and conversion’ (8.1 %–8.8 %) and ‘Amino acid transport and metabolism’ (7.5 %–9.0 %) had the largest proportions, except for functions “unknown”. Function ‘Cell wall/membrane/envelope biogenesis’ (6.8 %–7.4 %) was the third largest functional group in the upstream of site A3, but declined (6.4 %) to be less than function ‘Replication, recombination and repair’ (6.9 %) at site A3 (Fig. 3a). For potential functional genes with low proportions, including ‘Nuclear structure’, ‘Extracellular structures’ and ‘RNA processing and modification’, their abundance considerably changed with site, indicating that minor functional gene groups may be more seriously affected by metal pollution (Fig. 3b).

The spatial changes of carbon fixation pathway and nitrogen cycle pathway were obvious. The proportion of Calvin cycle near the spill site decreased (from 14.0 % at site B2 to 8.3 % at site A1) but then increased (to 16.4 % at site A3), which showed a similar change trend to Cyanobacteria

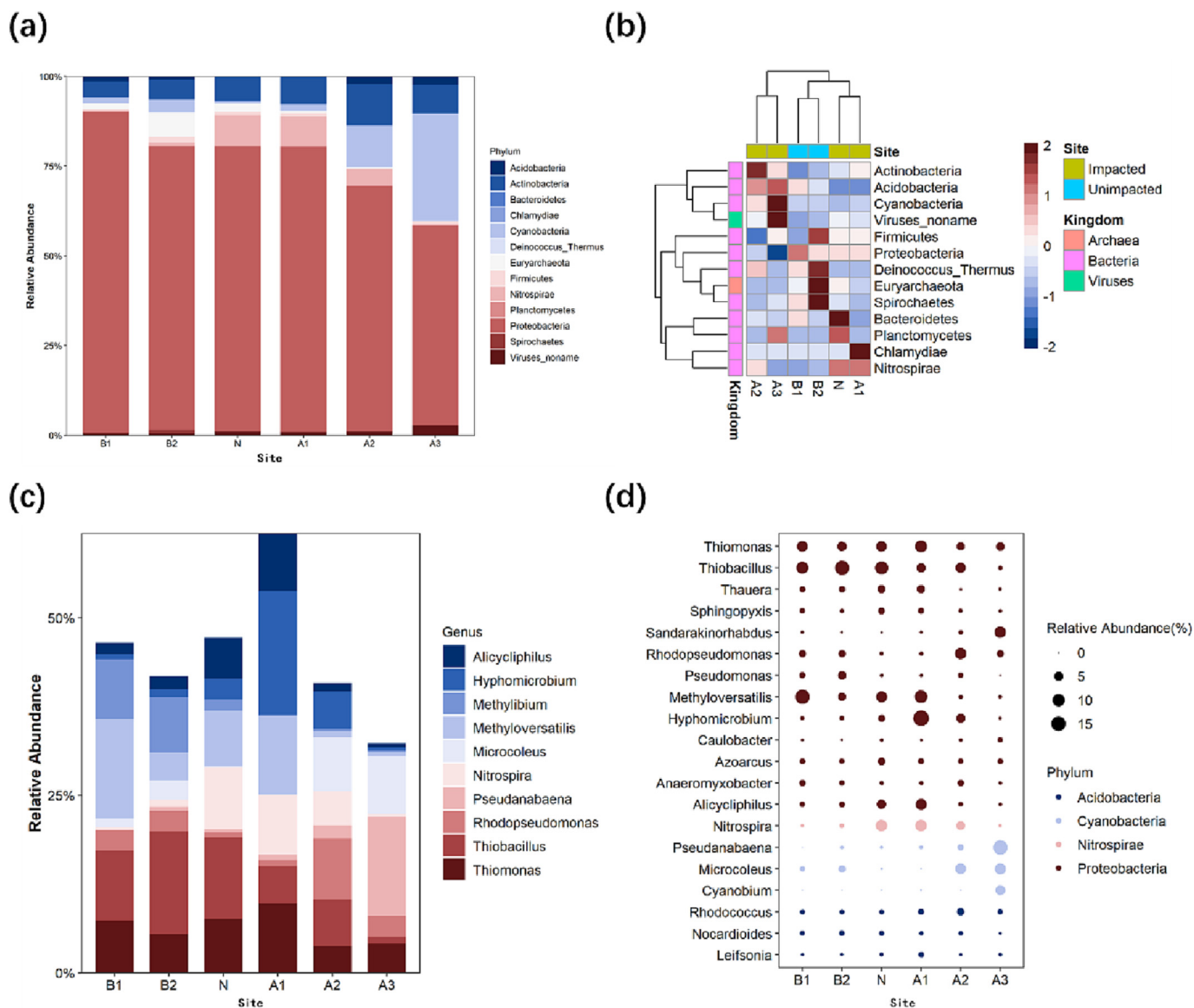


Fig. 2. Microbial community composition. Phylum-level composition (a) and inter-site comparison (b). Composition of the top 10 genera at all sites (c) and the top 20 genera at the contaminated sites (d).

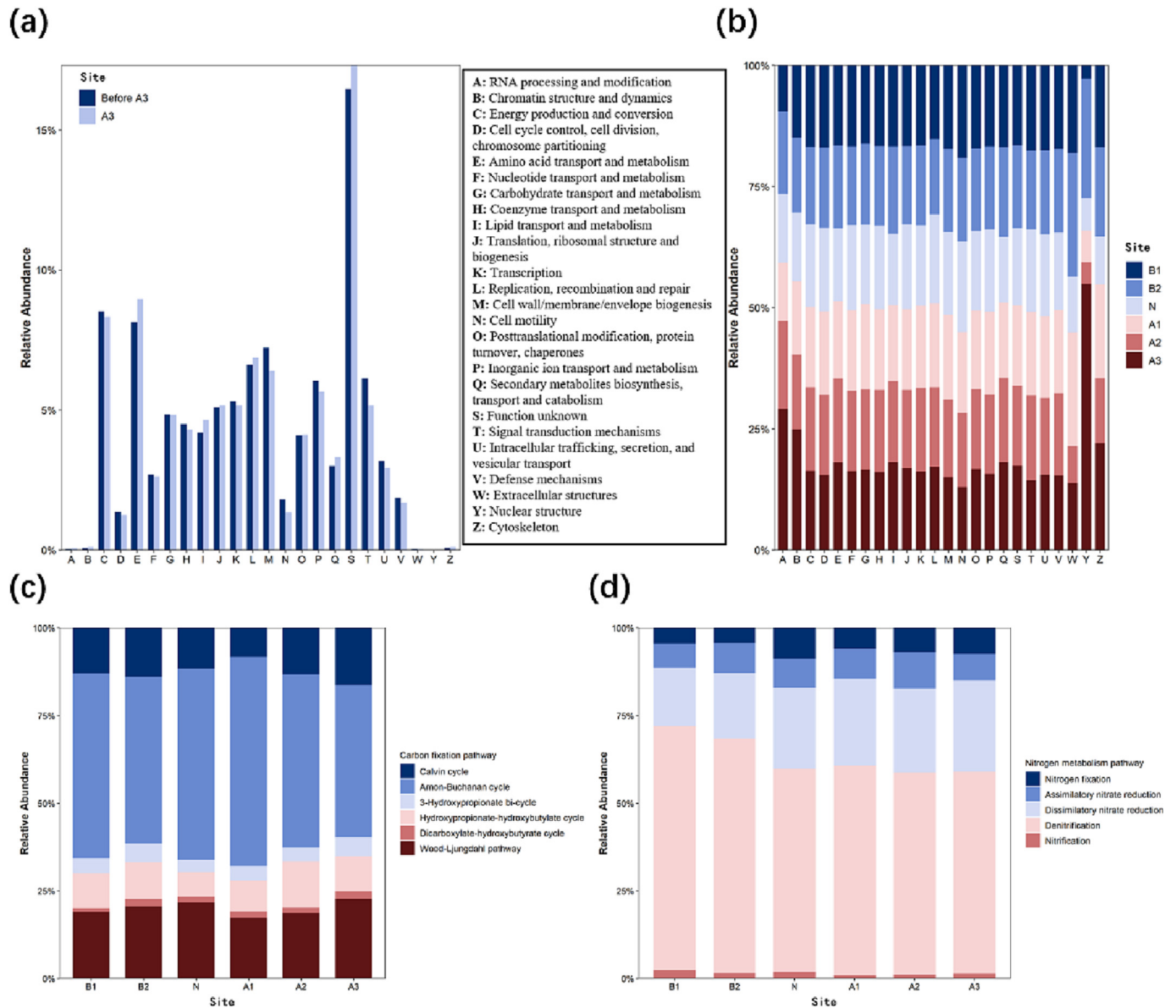


Fig. 3. Functional gene composition. COG classification of potential functional genes (a) and relative abundance at each site in each classification (b). The ratios of a given group to all groups in carbon fixation pathway (c) and nitrogen cycle pathway (d) potential genes.

(Fig. 3c). At metal-impacted sites, the proportion of nitrogen fixation pathway increased (from 4.3 % at site B2 to 8.8 % at site N), and the dissimilatory nitrate reduction increased (from 16.6 % at site B1 to 26.0 % at site A3), whereas denitrification decreased (from 69.7 % at site B1 to 57.6 % at site A3) in nitrogen removal pathway.

3.4. Profiles of MRGs and ARGs

A total of 29 subtypes belonging to 11 metal types of MRGs were annotated (Table S1), among which mercury resistance genes had the highest abundance (0.0012 %–0.0246 %). On the whole, MRGs were considerably enriched near the spill site (site N), but decreased with the river flow (Fig. 4a and b). Clustering analysis showed that similar MRGs structure was shared between background sites B1 and B2, and between contaminated sites N and A1, but a large difference existed not only between sites A2 and A3 but also between them and other sites (Fig. S5).

For ARGs, a total of 43 genes resistant to 10 antibiotics were annotated (Table S2). The overall trend of ARGs was first increasing but then

decreasing. The genes resistant to sulfonamides had the highest abundance (0.013 %–0.11 %) (Fig. 4c and d).

3.5. Correlations among environmental parameters, MRGs, ARGs and microbial composition

The correlations among environmental factors (e.g. NH_4^+ -N, TOC, pH and Tl concentration), MRGs, ARGs and microbial composition were deciphered (Table S3). MRGs and ARGs were not significantly correlated with Tl concentration ($p > 0.05$), but with water pH ($p < 0.01$) (Fig. 5a). There was a significant correlation between MRGs and ARGs ($p < 0.05$), with 46 nodes and 265 edges in the subtype co-occurrence network (Fig. 5b). There was a strong co-occurrence relationship among different ARGs subtypes, while for MRGs, it also existed only among subtypes with the same metal resistance. *mexF* and *pcoA* genes had the maximum number of connecting edges between MRGs and ARGs (18). *mexF* gene was identified as both multiple drug resistance gene and multiple heavy metal resistance gene, while *pcoA* gene was a copper resistance gene.

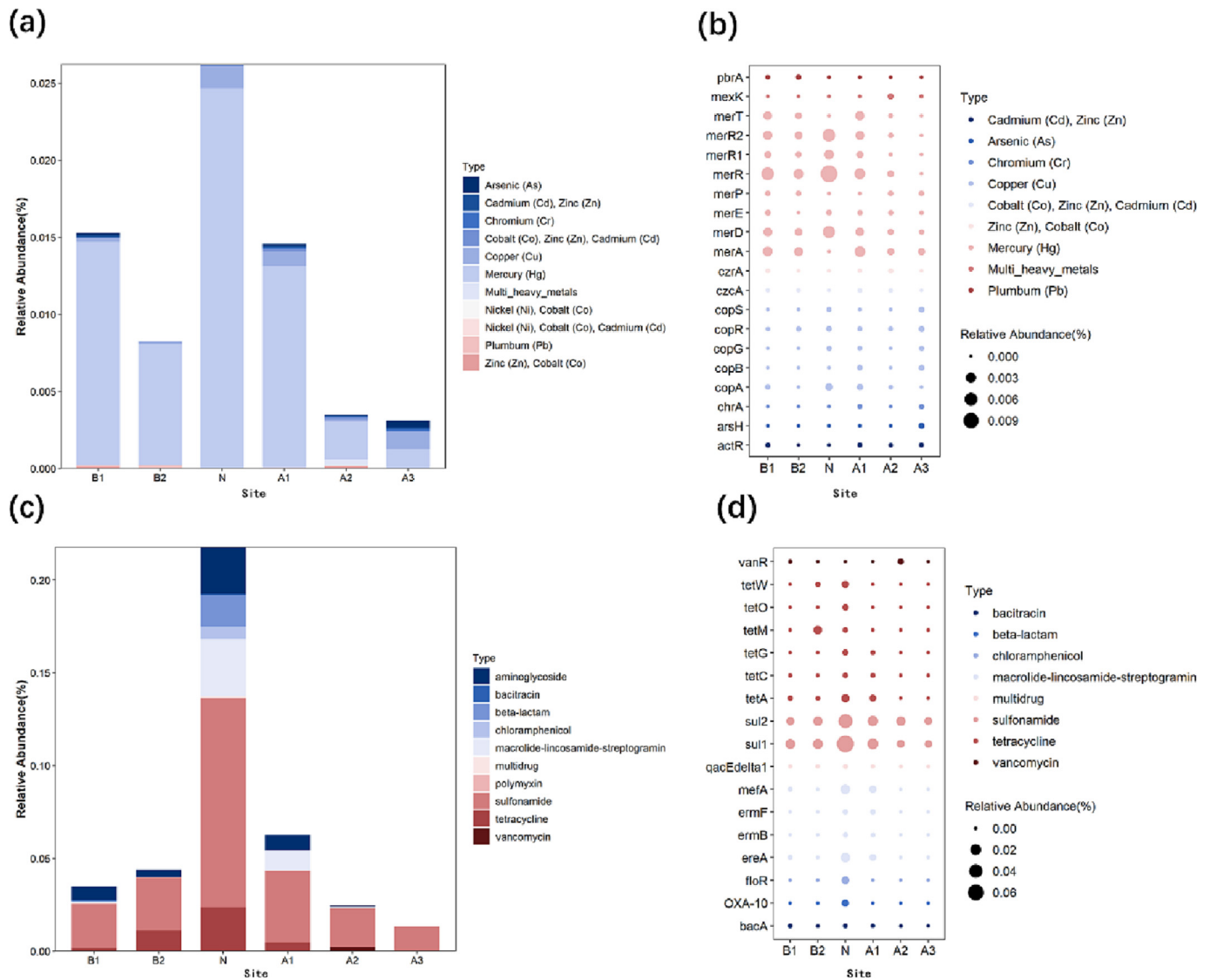


Fig. 4. Profiles of MRGs and ARGs. The relative abundance of MRGs (a) and ARGs (c) and the top 20 MRGs (b) and ARGs (d).

Apart from this, mercury resistance genes also had many linking edges, which were closely related with ARGs.

Two bacterial phyla were associated with resistance genes (Fig. 5c). Bacteroidetes was positively correlated with ARGs ($p < 0.05$), indicating that this phylum may carry ARGs, while Acidobacteria show a negative correlation with MRGs ($p < 0.05$). There was a positive correlation between Chlamydiae and sediment Tl concentration ($p < 0.001$), indicating that this phylum had a strong adaptability to Tl pollution. Besides, Acidobacteria and Bacteroidetes were correlated with water pH ($p < 0.05$), and Actinobacteria was correlated with water Tl concentration ($p < 0.01$) (Table. S4).

The co-occurrence network of microbial composition and MRG subtypes consisted of 88 nodes and 170 edges (Fig. 5d). There were 64 links between the MRGs and genera. The largest number of bacteria were associated with mercury resistance genes *merF* and *merR1*, including 6 genera within Proteobacteria and *Nitrospira* within Nitrospirae. *Sphingopyxis* within Proteobacteria had many connections with MRGs, suggesting that it may carry multiple heavy metal resistance genes. The co-occurrence network analysis of ARGs and microbial composition showed that *Bifidobacterium* within Actinobacteria was associated with the largest number of ARGs, followed by *Sphingopyxis*, *Azoarcus* and *Thauera* within Proteobacteria (Fig. S6).

4. Discussion

With the development of mining, smelting and other industries, metal incidents occur frequently. The response of microorganisms to Tl contamination in water, sediment and soil has been reported by many previous studies. However, most of these studies have selected samples with relatively low Tl concentration (the reported highest concentration < 16 mg/kg) and relatively low difference in Tl concentration was detected among samples (Chen et al., 2023; J. Liu et al., 2023; Wang et al., 2020), and the studies on samples with high Tl concentrations did not use metagenomic technology to analyze functional genes (Rasool et al., 2020; Rasool and Xiao, 2018; Sun et al., 2012). In this study, metagenomic sequencing was used to analyze the microbial composition and functional genes in the sediments impacted by a high variance of Tl concentration (0.87–41.5 mg/kg), in order to further elucidate the effect of Tl spill on sediment microbial community.

Since Tl and potassium (K) ion have similar ionic radii, the effect of Tl on microorganisms was likely due to that it mediates the K^+ involved process, thus causing cytotoxicity (Peter and Viraraghavan, 2005). Different microorganisms have different affinity for Tl and K uptake, so Tl has different impacts on different microorganisms. Microorganisms with higher affinity for Tl may absorb more Tl instead of K, resulting in the inhibition

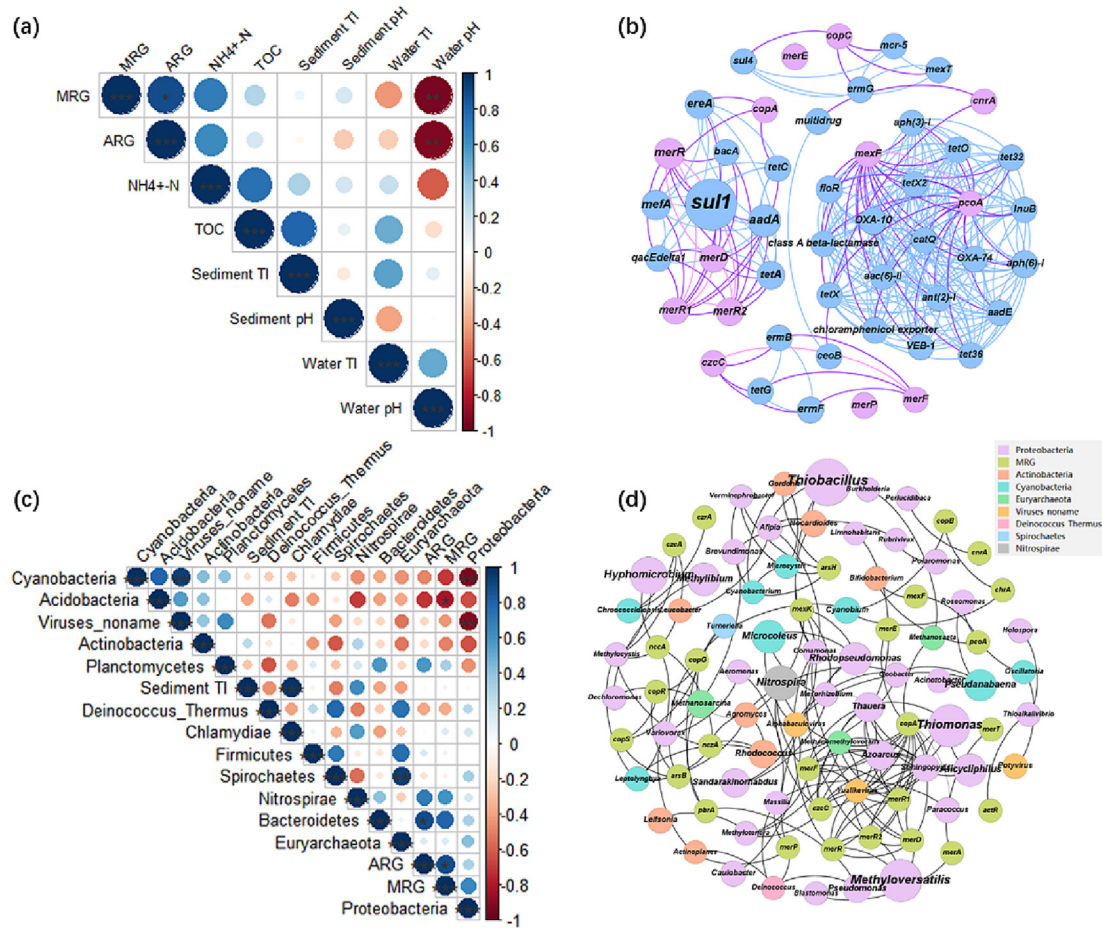


Fig. 5. Correlations among environmental parameters, MRGs, ARGs, and microbial composition. Pearson's correlation analysis of environmental parameters with MRGs and ARGs (a) and of sediment TI concentration, MRGs and ARGs with microbial phyla (c). Co-occurrence network analysis of between MRGs and ARGs (b) and between MRGs and microbial composition (d). In the correlation graph, * represents $p < 0.05$, ** represents $p < 0.01$, *** represents $p < 0.001$. In panel b, the connecting line between ARGs is blue, between MRGs is pink, and between ARGs and MRGs is purple.

of cellular processes involved in K, which affects microbial growth and even death (Norris et al., 1976). Therefore, the change of TI concentration in the environment will screen the local microorganisms, leading to changes in microbial composition and function.

In both TI spill-impacted environment and other metals spill-impacted environment, Proteobacteria abundance remained relatively high (Chen et al., 2022; Guo et al., 2019; Rasool and Xiao, 2018; She et al., 2022). Proteobacteria was the largest group of bacteria, which not only had a strong environmental adaptability, but also had certain resistance and repair ability to heavy metal pollution (J. Liu et al., 2023; Nwaehiri et al., 2020; Rasool et al., 2020). In this research, we also found that many proteobacterial organisms were associated with MRGs and ARGs, which suggested that they might harbor these resistance genes.

Our study found that Cyanobacteria abundance immediately became very low after exposure to a very serious TI pollution, and then gradually increased with the decreasing TI content. Except for the more severely polluted sites, the proportions of Cyanobacteria at spill-impacted sites exceeded considerably those at the background sites. Its resistance to metal pollution has also been confirmed in other previous studies (Chen et al., 2023; Wang et al., 2020). Many species of Cyanobacteria exhibited metal tolerance through extracellular binding precipitation, cellular impermeability and exclusion, and internal detoxification mechanisms (Fiore and Trevors, 1994). Moreover, Cyanobacteria have relatively stronger adaptability and resilience to the disturbance of environmental pressure due to their photosynthetic autotrophy (Barthes et al., 2015). Cyanobacteria harbors different intracellular metabolic fingerprints compared with

heterotrophic bacteria, demonstrating that phototrophic communities can gain advantages by using interwoven metabolic networks for division of labor (Zuniga et al., 2020).

Among the potential functional genes, the genes with very low relative abundance, namely “Nuclear structure” and “RNA processing and modification”, increased considerably at the contaminated sites. Nuclear structure was related to gene regulation mechanism (Stein, 1998). RNA processing and modification can change the relationship between RNA structure and function and various cellular processes (Novoa et al., 2017). The expression of these two relevant proteins was related to gene regulation and transcription. In the harsh environment, the expression of specific genes was likely different from that in the normal environment (Stein et al., 1996). Besides, Guo et al. documented that heavy metal spill could have a considerable impact on the abundance and richness of sediment denitrifier communities (Guo et al., 2018). Our research revealed that the abundance of denitrification functional genes decreased after exposure to TI pollution caused by accidental spill.

To date, no TI resistance genes has been documented, but several studies have shown that certain heavy metal contamination can screen microorganisms with other kinds of MRGs (Perron et al., 2004; Rasool and Xiao, 2018). Moreover, many studies also have shown that the environment polluted by heavy metals can not only screen out microorganisms carrying MRGs, but also had a certain screening effect on ARGs-carrying microorganisms (Gupta et al., 2023; Squadrone, 2020; Sun et al., 2021). Therefore, the correlation between MRGs and ARGs had been documented in many previous studies (Anderson et al., 2017; Di Cesare et al., 2016; Imran

et al., 2019). Through database comparison and co-occurrence network analysis, we also found that MRGs and ARGs were co-existent and correlated at T1 contaminated sites, in line with the results of other studies on the sediments impacted by T1 spill (Chen et al., 2023; Wang et al., 2020). They simultaneously accumulated in sediments after exposure to sudden serious contamination and then gradually decreased in the downstream.

In no harmony with other studies (J.W. Chen et al., 2019; Chen et al., 2023; Gupta et al., 2023), there was no significant correlation between MRGs/ARGs and T1 concentration in this study ($r = 0.06$), but a negative correlation was detected between MRGs/ARGs and water pH, which was consistent with the result of J.W. Chen et al. (2019). For the relationship between pollution and resistance genes, a previous study pointed out that the abundance of MRGs was higher at both lightly and highly metal contaminated sites, but lower at moderate contaminated sites, which indicated that there was a complex relationship between environmental variables and the functional structure of microbial community in natural environment (Waldron et al., 2009). For the effect of pH on resistance genes, different resistance genes have their own suitable environment. Some previous studies showed that acidic conditions were not favorable for ARGs-carrying bacteria (Lin et al., 2020; Yang et al., 2014; Yu et al., 2023), while others found that alkaline conditions could reduce resistance genes (J.W. Chen et al., 2019; Y.G. Chen et al., 2019; Huang et al., 2016). There was little change in water pH in this study (<1), and the closer to neutral conditions, the higher the abundance of resistance genes, which was consistent with the two previous studies (J.W. Chen et al., 2019; Y.G. Chen et al., 2019; Lin et al., 2020). Furthermore, with more data, Z.S. Liu et al. (2023) used metagenomic analysis to reveal the deterministic role of pH in shaping resistance groups in soil, and they indicated that soil pH played a decisive role in the formation of ARGs characteristics.

Co-occurrence network analysis showed that *Sphingopyxis* was associated with the largest number of MRGs and ARGs, suggesting that it may be the main host of resistance genes. *Sphingopyxis* was an extensively studied genus with 31 child taxa studied and published so far (<https://lpsn.dsmz.de/genus/sphingopyxis>). It can grow in many ecological niches, including harsh environments, so that it has acquired many genes and metabolic pathways adapted to the environment (Sharma et al., 2021). Some species of *Sphingopyxis* can not only survive in metal-polluted environments, but also had an ability to degrade metals (Liang et al., 2016; Mahbub et al., 2017). In addition, *Sphingopyxis* can be acclimatized to and degrade antibacterial substances, such as berberine for sp. B16 (S.Y. Liu et al., 2019) and triclosan for sp. KCY1 (Lee et al., 2012).

5. Conclusions

We explored the microbial community compositions and functions of T1 spill-impacted and unimpacted sediments using metagenomics assay. Proteobacteria were the most abundant, while Cyanobacteria also had a strong resistance. At the genus level, *Hyphomicrobium*, *Thiomonas* and *Alicyclophilus* dominated in T1-contaminated sediments. The abundance of functional genes 'Nuclear structure' and 'RNA processing and modification' in T1 spill-impacted sediments increased. The Calvin cycle in the carbon fixation pathway decreased first and then increased. The abundance of nitrogen fixing genes increased, while the abundance of denitrification genes decreased. MRGs and ARGs were correlated with each other, and they were significantly correlated with water pH. *Sphingopyxis* has the highest correlation with resistance genes and may be the main host carrying resistance genes in T1-contaminated environment.

CRedit authorship contribution statement

Shuang Yan: Conceptualization, Methodology, Writing - original draft. **Zhengke Zhang:** Methodology, Formal analysis. **Ji Wang:** Methodology, Formal analysis. **Yulin Xia:** Methodology, Data analysis. **Sili Chen:** Conceptualization, Supervision, Writing-review & editing. **Shuguang Xie:** Conceptualization, Supervision.

Data availability

Data will be made available on request.

Declaration of competing interest

The authors declare that they have no known competing financial interests or personal relationships that could have appeared to influence the work reported in this paper.

Acknowledgments

This work was financially supported by National Key Research and Development Program (2022YFC3705004). Data processing was supported by the High-performance Computing Platform of Peking University.

Appendix A. Supplementary data

Supplementary data to this article can be found online at <https://doi.org/10.1016/j.scitotenv.2023.163101>.

References

- Anderson, L.G., Xia, Y., Zhang, T., 2017. Co-occurrence of antibiotic and metal resistance genes revealed in complete genome collection. *ISME J.* 11, 651–662.
- Barthes, A., Ten-Hage, L., Lamy, A., Rols, J.L., Lefflaive, J., 2015. Resilience of microbial communities subjected to drought—small-scale studies. *Microb. Ecol.* 70, 9–20.
- Belzile, N., Chen, Y.W., 2017. Thallium in the environment: a critical review focused on natural waters, soils, sediments and airborne particles. *Appl. Geochem.* 84, 218–243.
- Bennett, B.D., Brutinel, E.D., Gralnick, J.A., 2015. A ferrous iron exporter mediates iron resistance in *Shewanella oneidensis* MR-1. *Appl. Environ. Microbiol.* 81, 7938–7944.
- Bolger, A.M., Lohse, M., Usadel, B., 2014. Trimmomatic: a flexible trimmer for illumina sequence data. *Bioinformatics* 30, 2114–2120.
- Campanella, B., Colombaioni, L., Benedetti, E., Di Ciaglia, A., Ghezzi, L., Onor, M., D'Orazio, M., Giannecchini, R., Petrini, R., Bramanti, E., 2019. Toxicity of thallium at low doses: a review. *Int. J. Environ. Res. Public Health* 16, 4732.
- Cantalapiedra, C.P., Hernandez-Plaza, A., Letunic, I., Bork, P., Huerta-Cepas, J., 2021. eggNOG-mapper v2: functional annotation, orthology assignments, and domain prediction at the metagenomic scale. *Mol. Biol. Evol.* 38, 5825–5829.
- Chen, J.W., Li, J.J., Zhang, H., Shi, W., Liu, Y., 2019. Bacterial heavy-metal and antibiotic resistance genes in a copper tailing dam area in northern China. *Front. Microbiol.* 10, 1916.
- Chen, X.L., Wang, J., Pan, C.Y., Feng, L.S., Chen, S.L., Xie, S.G., 2023. Metagenomic insights into the influence of thallium spill on sediment microbial community. *Environ. Pollut.* 317, 120660.
- Chen, X.L., Wang, J., Pan, C.Y., Feng, L.S., Guo, Q.W., Chen, S.L., Xie, S.G., 2022. Metagenomic analysis reveals the response of microbial community in river sediment to accidental antimony contamination. *Sci. Total Environ.* 813, 152484.
- Chen, Y.G., Huang, H.N., Zheng, X., 2019. Fate of sulfonamide resistance genes during sludge anaerobic fermentation: roles of sludge components and fermentation pHs. *Bioresour. Technol.* 289, 121636.
- Csardi, G., Nepusz, T., 2006. The igraph software package for complex network research. *InterJ. Complex Syst.*, 1695. <https://igraph.org>.
- Di Cesare, A., Eckert, E.M., D'Urso, S., Bertoni, R., Gillan, D.C., Wattiez, R., Corno, G., 2016. Co-occurrence of integrase 1, antibiotic and heavy metal resistance genes in municipal wastewater treatment plants. *Water Res.* 94, 208–214.
- Fiore, M.F., Trevors, J.T., 1994. Cell composition and metal tolerance in cyanobacteria. *Biomol. J.* 7, 83–103.
- Fu, L.M., Niu, B.F., Zhu, Z.W., Wu, S.T., Li, W.Z., 2012. CD-HIT: accelerated for clustering the next-generation sequencing data. *Bioinformatics* 28, 3150–3152.
- Guo, Q.W., Li, N.N., Bing, Y.X., Chen, S.L., Zhang, Z.K., Chang, S., Chen, Y., Xie, S.G., 2018. Denitrifier communities impacted by heavy metal contamination in freshwater sediment. *Environ. Pollut.* 242, 426–432.
- Guo, Q.W., Li, N., Xie, S.G., 2019. Heavy metal spill influences bacterial communities in freshwater sediments. *Arch. Microbiol.* 201, 847–854.
- Gupta, S., Graham, D.W., Sreekrishnan, T.R., Ahammad, S.Z., 2023. Heavy metal and antibiotic resistance in four Indian and UK rivers with different levels and types of water pollution. *Sci. Total Environ.* 857, 159059.
- Gurevich, A., Saveliev, V., Vyahhi, N., Tesler, G., 2013. QUASt: quality assessment tool for genome assemblies. *Bioinformatics* 29, 1072–1075.
- Huang, H.N., Chen, Y.G., Zheng, X., Su, Y.L., 2016. Distribution of tetracycline resistance genes in anaerobic treatment of waste sludge: the role of pH in regulating tetracycline resistant bacteria and horizontal gene transfer. *Bioresour. Technol.* 218, 1284–1289.
- Huerta-Cepas, J., Szklarczyk, D., Heller, D., Hernandez-Plaza, A., Forslund, S.K., Cook, H., Mende, D.R., Letunic, I., Rattei, T., Jensen, L.J., von Mering, C., Bork, P., 2019. eggNOG 5.0: a hierarchical, functionally and phylogenetically annotated orthology resource based on 5090 organisms and 2502 viruses. *Nucleic Acids Res.* 47, D309–D314.
- Imran, Md., Das, K.R., Naik, M.M., 2019. Co-selection of multi-antibiotic resistance in bacterial pathogens in metal and microplastic contaminated environments: an emerging health threat. *Chemosphere* 215, 846–857.

- Karbowska, B., 2016. Presence of thallium in the environment: sources of contaminations, distribution and monitoring methods. *Environ. Monit. Assess.* 188, 640.
- Kolde, Raivo, 2019. pheatmap: pretty heatmaps. R package version 1.0.12. <https://CRAN.R-project.org/package=pheatmap>.
- Langmead, B., Salzberg, S.L., 2012. Fast gapped-read alignment with bowtie 2. *Nat. Methods* 9, 357–U54.
- Lee, D.G., Zhao, F.M., Rezenom, Y.H., Russell, D.H., Chu, K.H., 2012. Biodegradation of triclosan by a wastewater microorganism. *Water Res.* 46, 4226–4234.
- Li, D.D., Xu, X.J., Yu, H.W., Han, X.R., 2017. Characterization of Pb²⁺ biosorption by psychrotrophic strain *Pseudomonas* sp. I3 isolated from permafrost soil of mohe wetland in Northeast China. *J. Environ. Manag.* 196, 8–15.
- Li, D.H., Liu, C.M., Luo, R.B., Sadakane, K., Lam, T.W., 2015. MEGAHIT: an ultra-fast single-node solution for large and complex metagenomics assembly via succinct de bruijn graph. *Bioinformatics* 31, 1674–1676.
- Li, Y.B., Zhang, M.M., Xu, R., Lin, H.Z., Sun, X.X., Xu, F.Q., Gao, P., Kong, T.L., Xiao, E.Z., Yang, N.L., Sun, W.M., 2021. Arsenic and antimony co-contamination influences on soil microbial community composition and functions: relevance to arsenic resistance and carbon, nitrogen, and sulfur cycling. *Environ. Int.* 153, 106522.
- Liang, J.S., Bai, Y.H., Hu, C.Z., Qu, J.H., 2016. Cooperative Mn(II) oxidation between two bacterial strains in an aquatic environment. *Water Res.* 89, 252–260.
- Lin, H., Sun, W.C., Yu, Q.G., Ma, J.W., 2020. Acidic conditions enhance the removal of sulfonamide antibiotics and antibiotic resistance determinants in swine manure. *Environ. Pollut.* 263 (A), 114629.
- Liu, J., Luo, X.W., Sun, Y.Q., Tsang, D.C.W., Qi, J.Y., Zhang, W.L., Li, N., Yin, M.L., Wang, J., Lippold, H., Chen, Y.H., Sheng, G.D., 2019a. Thallium pollution in China and removal technologies for waters: a review. *Environ. Int.* 126, 771–790.
- Liu, J., Wan, Y.B., Wei, X.D., She, J.Y., Ouyang, Q.E., Deng, P.Y., Hu, H.Y., Zhang, X.Y., Fang, M.Y., Wei, X.L., Liu, W.F., Gong, J., Wang, J., 2023a. Microbial diversity in paddy rhizospheric soils around a large industrial thallium-containing sulfide utilization zone. *Environ. Res.* 216, 114627.
- Liu, J., Wang, J., Chen, Y.H., Lippold, H., Xiao, T.F., Li, H.S., Shen, C.C., Xie, L.H., Xie, X.F., Yang, H.L., 2017. Geochemical transfer and preliminary health risk assessment of thallium in a riverine system in the Pearl River Basin, South China. *J. Geochem. Explor.* 176, 64–75.
- Liu, S.Y., Zhang, Y., Zeng, P., Wang, H.L., Song, Y.H., Li, J., 2019b. Isolation and characterization of a bacterial strain capable of efficient berberine degradation. *Int. J. Environ. Res. Public Health* 16, 646.
- Liu, Z.S., Zhao, Y.X., Zhang, B.F., Wang, J.Q., Zhu, L.Z., Hu, B.L., 2023b. Deterministic effect of pH on shaping soil resistome revealed by metagenomic analysis. *Environ. Sci. Technol.* 57, 985–996.
- Mahbub, K.R., Krishnan, K., Megharaj, M., Naidu, R., 2016. Bioremediation potential of a highly mercury resistant bacterial strain *Sphingobium* SA2 isolated from contaminated soil. *Chemosphere* 144, 330–337.
- Mahbub, K.R., Krishnan, K., Naidu, R., Megharaj, M., 2017. Mercury remediation potential of a mercury resistant strain *Sphingopyxis* sp. SE2 isolated from contaminated soil. *J. Environ. Sci.* 51, 128–137.
- Manasi, Rajesh V., Rajesh, N., 2015. An indigenous *Halomonas* BVR1 strain immobilized in crosslinked chitosan for adsorption of lead and cadmium. *Int. J. Biol. Macromol.* 79, 300–308.
- Mota, R., Pereira, S.B., Meazzini, M., Fernandes, R., Santos, A., Evans, C.A., De Philippis, R., Wright, P.C., Tamagnini, P., 2015. Effects of heavy metals on *Cyanothece* sp. CCY 0110 growth, extracellular polymeric substances (EPS) production, ultrastructure and protein profiles. *J. Proteome* 120, 75–94.
- Norris, P., Man, W.K., Hughes, M.N., Kelly, D.P., 1976. Toxicity and accumulation of thallium in bacteria and yeast. *Arch. Microbiol.* 110, 279–286.
- Novoa, E.M., Mason, C.E., Mattick, J.S., 2017. Charting the unknown epitranscriptome. *Nat. Rev. Mol. Cell Biol.* 18, 339–340.
- Nwaehiri, U.L., Akwukwaegbu, P.I., Bright Nwoke, B.E., 2020. Bacterial remediation of heavy metal polluted soil and effluent from paper mill industry. *Environ. Anal. Health Toxicol.* 35, e2020009.
- Pal, C., Bengtsson-Palme, J., Rensing, C., Kristiansson, E., Larsson, D.G.J., 2014. BacMet: antibacterial biocide and metal resistance genes database. *Nucleic Acids Res.* 42, D737–D743.
- Patro, R., Duggal, G., Love, M.I., Irizarry, R.A., Kingsford, C., 2017. Salmon provides fast and bias-aware quantification of transcript expression. *Nat. Methods* 14, 417–419.
- Perron, K., Caille, O., Rossier, C., van Delden, C., Dumas, J.L., Kohler, T., 2004. CzcR-CzcS, a two-component system involved in heavy metal and carbapenem resistance in *Pseudomonas aeruginosa*. *J. Biol. Chem.* 279, 8761–8768.
- Petrini, R., Cidu, R., Slejko, F.F., 2016. Thallium contamination in the raibl mine site stream drainage system (Eastern Alps, Italy). *Mine Water Environ.* 35, 55–63.
- Peter, A.L.J., Viraraghavan, T., 2005. Thallium: a review of public health and environmental concerns. *Environ. Int.* 31, 493–501.
- Pi, H.L., Patel, S.J., Arguello, J.M., Helmann, J.D., 2016. The *Listeria monocytogenes* fur-regulated virulence protein FrvA is an Fe(II) efflux P1B4-type ATPase. *Mol. Microbiol.* 100, 1066–1079.
- Rasool, A., Nasim, W., Xiao, T.F., Ali, W., Shafeeqe, M., Sultana, S.R., Fahad, S., Munis, M.F.H., Chaudhary, H.J., 2020. Microbial diversity response in thallium polluted river-bank soils of the lamuchang. *Ecotoxicol. Environ. Saf.* 187, 109854.
- Rasool, A., Xiao, T.F., 2018. Response of microbial communities to elevated thallium contamination in river sediments. *Geomicrobiol. J.* 35, 854–868.
- Revelle, W., 2021. psych: procedures for personality and psychological research. Northwestern University, Evanston, Illinois, USA. <https://CRAN.R-project.org/package=psych>.
- Rodriguez-Mercado, J.J., Mosqueda-Tapia, G., Altamirano-Lozano, M.A., 2017. Genotoxicity assessment of human peripheral lymphocytes induced by thallium(I) and thallium(III). *Toxicol. Environ. Chem.* 99, 987–998.
- Seemann, T., 2014. Prokka: rapid prokaryotic genome annotation. *Bioinformatics* 30, 2068–2069.
- Segata, N., Waldron, L., Ballarini, A., Narasimhan, V., Jousson, O., Huttenhower, C., 2012. Metagenomic microbial community profiling using unique clade-specific marker genes. *Nat. Methods* 9, 811–814.
- Sharma, M., Khurana, H., Singh, D.N., Negi, R.K., 2021. The genus *Sphingopyxis*: systematics, ecology, and bioremediation potential - a review. *J. Environ. Manag.* 280, 111744.
- She, J.Y., Liu, J., He, H.P., Zhang, Q., Lin, Y.Y., Wang, J., Yin, M.L., Wang, L.L., Wei, X.D., Huang, Y.L., Chen, C.Z., Lin, W.L., Chen, N., Xiao, T.F., 2022. Microbial response and adaptation to thallium contamination in soil profiles. *J. Hazard. Mater.* 423, 127080.
- Squadron, S., 2020. Water environments: metal-tolerant and antibiotic-resistant bacteria. *Environ. Monit. Assess.* 192, 238.
- Stein, G.S., 1998. Interrelationships of nuclear architecture with gene expression: functional encounters on a long and winding road. *J. Cell. Biochem.* 70, 157–158.
- Stein, G.S., Stein, J.L., Lian, J.B., vanWijnen, A.J., Montecino, M., 1996. Functional interrelationships between nuclear structure and transcriptional control: contributions to regulation of cell cycle- and tissue-specific gene expression. *J. Cell. Biochem.* 62, 198–209.
- Sun, F.L., Xu, Z.T., Fan, L.L., 2021. Response of heavy metal and antibiotic resistance genes and related microorganisms to different heavy metals in activated sludge. *J. Environ. Manag.* 300, 113754.
- Sun, J.L., Zou, X., Ning, Z.P., Sun, M., Peng, J.Q., Xiao, T.F., 2012. Culturable microbial groups and thallium-tolerant fungi in soils with high thallium contamination. *Sci. Total Environ.* 441, 258–264.
- Wei, T.Y., Simko, V., 2021. R package 'corrplot': visualization of a correlation matrix (version 0.90). <https://github.com/taiyun/corrplot>.
- Waldron, P.J., Wu, L.Y., Van Nostrand, J.D., Schadt, C.W., He, Z.L., Watson, D.B., Jardine, P.M., Palumbo, A.V., Hazen, T.C., Zhou, J.Z., 2009. Functional gene array-based analysis of microbial community structure in groundwaters with a gradient of contaminant levels. *Environ. Sci. Technol.* 43, 3529–3534.
- Wang, J., She, J.Y., Zhou, Y.C., Tsang, D.C.W., Beiyuan, J., Xiao, T.F., Dong, X.J., Chen, Y.H., Liu, J., Tin, M.L., Wang, L.L., 2020. Microbial insights into the biogeochemical features of thallium occurrence: a case study from polluted river sediments. *Sci. Total Environ.* 739, 139957.
- Wang, J., Wang, L.L., Wang, Y.X., Tsang, D.C.W., Yang, X., Beiyuan, J.Z., Yin, M.L., Xiao, T.F., Jiang, Y.J., Lin, W.L., Zhou, Y.C., Liu, J., Wang, L., Zhao, M., 2022. Emerging risks of toxic metal(loid)s in soil-vegetables influenced by steel-making activities and isotopic source apportionment. *Environ. Int.* 146, 106207.
- Wickham, H., 2016. ggplot2: Elegant Graphics for Data Analysis. Springer-Verlag, New York.
- Xu, X.J., Li, H.Y., Wang, Q.Y., Li, D.D., Han, X.R., Yu, H.W., 2017. A facile approach for surface alteration of *Pseudomonas putida* I3 by supplying K₂SO₄ into growth medium: enhanced removal of Pb(II) from aqueous solution. *Bioresour. Technol.* 232, 79–86.
- Yang, C.W., Chang, Y.T., Chao, W.L., Shiung, L.L., Lin, H.S., Chen, H., Ho, S.H., Lu, M.J., Lee, P.H., Fan, S.N., 2014. An investigation of total bacterial communities, culturable antibiotic-resistant bacterial communities and integrons in the river water environments of Taipei City. *J. Hazard. Mater.* 277, 159–168.
- Yin, X.L., Jiang, X.T., Chai, B.L., Li, L.G., Yang, Y., Cole, J.R., Tiedje, J.M., Zhang, T., 2018. ARGs-OAP v2.0 with an expanded SARG database and hidden markov models for enhancement characterization and quantification of antibiotic resistance genes in environmental metagenomes. *Bioinformatics* 34, 2263–2270.
- Yu, P., Dong, P.Y., Zou, Y.N., Wang, H., 2023. Effect of pH on the mitigation of extracellular/intracellular antibiotic resistance genes and antibiotic resistance pathogenic bacteria during anaerobic fermentation of swine manure. *Bioresour. Technol.* 373, 128706.
- Zuniga, C., Li, T.T., Guarnieri, M.T., Jenkins, J.P., Li, C.T., Bingol, K., Kim, Y.M., Betenbaugh, M.J., Zengler, K., 2020. Synthetic microbial communities of heterotrophs and phototrophs facilitate sustainable growth. *Nat. Commun.* 11, 3803.